T. RATAJSKI*#, I. KALEMBA-REC*, B. DUBIEL*

INFLUENCE OF PAA ON THE MICROSTRUCTURE AND CORROSION RESISTANCE OF ELECTROPHORETICALLY DEPOSITED SiO$_2$ AND Ni/SiO$_2$ COATINGS ON X2CrNiMo17-12-2 STEEL

The effect of anionic surfactant in the form of polyacrylic acid (PAA) on the electrophoretic deposition of the SiO$_2$ and Ni/SiO$_2$ coatings on X2CrNiMo17-12-2 stainless steel was examined. Parameters of the process, such as chemical composition of the suspensions, voltage between the electrodes and the deposition time were experimentally selected. Zeta potential measurements showed a beneficial effect of polyacrylic acid on the SiO$_2$ and Ni particles stability in ethanol. Scanning and transmission electron microscopy studies revealed that the microstructure of the coatings obtained from the suspensions containing polyelectrolyte is more homogenous and has less amount of desiccation cracks on the surface. The results of the polarization tests have shown that addition of anionic surfactant improves also corrosion resistance of the coatings in 3.5% NaCl solution.

Keywords: electrophoretic deposition (EPD), electrosteric stabilization, SiO$_2$ coatings, nanocomposite Ni/SiO$_2$ coatings, PAA

1. Introduction

Electrophoretic deposition method (EPD) can be useful for preparation various coatings on conductive substrates [1-5]. For deposition of such coatings very often suspensions without water are used to prevent hydrolysis and producing hydrogen on the cathode [6].

One of the problems in electrophoretic deposition of uniform coatings is low stability of suspended particles and high degree of agglomeration. Nanoparticles have stronger tendency to agglomeration than micrometre size particles due to the occurrence of van der Waals forces between them [7]. These forces can be counterbalanced by the electrostatic and steric stabilization [8]. Electrostatic stabilization is achieved by changing the pH of the suspension, which in turn influences the change of the particles charge [9]. Steric stabilization requires the use of surfactant, which adsorbs on the surface of nanoparticles and forms a thin layer which prevents agglomeration [10-12]. In general, combination of both types of stabilization is called electrosteric stabilization [13]. It can be achieved for example by using polyelectrolyte. One of the substances used to stabilize the oxides suspensions is polyacrylic acid ((C$_3$H$_4$O$_2$)$_n$) [14].

Surfactants can exert positive influence on the electrophoretic deposition and properties of the coatings by increasing their homogeneity. One of the applications, which requires compact surface, are corrosion resistant coatings for protection of austenitic stainless steels in environments containing Cl$^-$ ions. Among them, oxide and nanocomposite coatings have attracted much attention. Particularly noteworthy are SiO$_2$ coatings [15, 16], as well as oxide matrix composite coatings like Ni/SiO$_2$ [17]. This type of coatings exhibits good corrosion resistance and high mechanical properties. In addition, coatings containing nickel can be used as components of catalysts [18]. Literature reports exhibit the possibility of the use of PAA for electrophoretic deposition of pure SiO$_2$ coatings [19, 20]. Unfortunately, there is still lack of information confirming the positive influence of this anionic surfactant on the stability and deposition behaviour of composite coatings.

The aim of this work was to investigate the influence of PAA on the zeta potential of SiO$_2$ and Ni particles in ethanol-based suspensions and to determine the parameters of the electrophoretic deposition of SiO$_2$ and Ni/SiO$_2$ coatings with surfactant on X2CrNiMo17-12-2 stainless steel. Their microstructure, surface topography and potentiodynamic polarization in 3.5% aqueous NaCl solution were also examined.

2. Materials and methods

As a substrate for coatings' deposition rectangular plates (15 mm × 30 mm) from X2CrNiMo17-12-2 stainless steel were used. As a counter electrode the same steel with dimensions 60 mm × 30 mm was applied. The electrodes were placed 10 mm from each other in glass cell. Before EPD, the working surfaces were grinded with sandpaper of 2000 grit and then cleaned with distilled water and ethanol.

*   AGH UNIVERSITY OF SCIENCE AND TECHNOLOGY, FACULTY OF METALS ENGINEERING AND INDUSTRIAL COMPUTER SCIENCE, AL.MICKIEWICZA 30, 30-059 KRAKÓW, POLAND

Corresponding author: ratajski@agh.edu.pl

2074

For electrophoretic deposition of SiO_2 and Ni/SiO_2 coatings ethanol-based suspensions with SiO_2 and Ni particles were used. SiO_2 nanoparticles with average diameter equal to 23 ± 7 nm and nickel particles with diameter equal to 464 ± 129 nm were delivered by Sigma-Aldrich. Equivalent circle diameters were estimated from areas of the particles measured on TEM images. Based on the measurements results, the mean diameters and the standard deviations were calculated. In order to investigate the influence of anionic surfactant on the electrophoretic deposition mechanism, ethanol based suspensions containing also PAA were used. Molecular weight of the polyelectrolyte was equal to 1800 g/mol. The influence of pH on suspensions stability was examined by adding acetic acid and ammonia. To each suspension, with concentrations of SiO_2 particles in ethanol from 0.8 g/L to 1.6 g/L, the 0.1 wt% of PAA was also added. In order to deposit nanocomposite Ni/SiO_2 coatings, the similar suspensions as used for SiO_2 deposition, additionally containing 5 g/L and 15 g/L of Ni powder were prepared. Before deposition suspensions were ultrasonically dispersed for one hour and then stirred also for one hour in order to separate and obtain an even distribution of particles in ethanol.

Trial series of coatings were deposited using constant applied voltage in the range from 5 V to 90 V and deposition time from 60 s to 420 s. After EPD received coatings were dried at room temperature.

For determination of the stability of the particles suspended in ethanol, zeta potential measurements were performed by means of Malvern Zetasizer Nano ZS90. The changes of suspensions pH were realized by addition of acetic acid and ammonia water and measured by means of Mettler Toledo pH meter.

Macroscopic inspections of coatings quality were focused on the observations of such defects like an uneven thickness, cracks and voids.

Microstructural investigation was carried out using scanning electron microscope (SEM) FEI Nova NanoSEM 450 using plan view and cross-section specimens. SEM images were acquired with the use of secondary electron detector (SE) and circular backscatter electron detector (BSE) with the electron beam accelerating voltage of 10 kV.

Transmission electron microscopy (TEM) investigation was performed using Jeol JEM-2010 ARP microscope using the plan-view samples from electrophoretically deposited coatings. Phase analysis of the coatings' components was performed using selected area electron diffraction (SAED) and characteristic X-ray energy dispersive spectrometry (EDS).

Surface topography was measured using optical profilometer Veeco WYKO NT930.

The corrosion resistance was investigated by open circuit potential measurements and polarization test in 3.5% NaCl solution by means of Autolab Potentiostat/Galvanostat PG-STAT302N. Measurements were carried out at potential range from -0.6 V to 1.6 V and scan rate equal to 0.001 V/s. Platinum plate was used as a counter electrode. Corrosion potential and current were estimated using Tafel extrapolation method.

3. Results and discussion

3.1. Deposition of SiO_2 and Ni/SiO_2 coatings

The most important parameter which describes the stability, as well as indirectly mobility of the particles in suspension, is the electrokinetic potential (zeta potential). Figures 1 and 2 show the relationship between zeta potential and pH for SiO_2 and Ni/SiO_2 suspensions, also with the addition of 0.1% of PAA, respectively. In both cases anionic surfactant shifts the isoelectric point to lower pH values. Furthermore, PAA affects also on the zeta potential, what in consequence influences the improvement of the stability of the particles in ethanol-based suspension.

For SiO_2 coatings deposition suspension with pH equal to 6.97 and zeta potential equal to -11.6 mV (Table 1) was selected. At higher pH values, despite the increase of zeta potential, the deterioration of the homogeneity of the coatings was observed. Addition of PAA, due to improvement of the stability, allowed to use suspension with zeta potential equal to -60.3 at pH equal to 11.3. For both suspensions, despite an increase of the particles stability at higher pH values, the obtained coatings were macroscopically inhomogeneous.
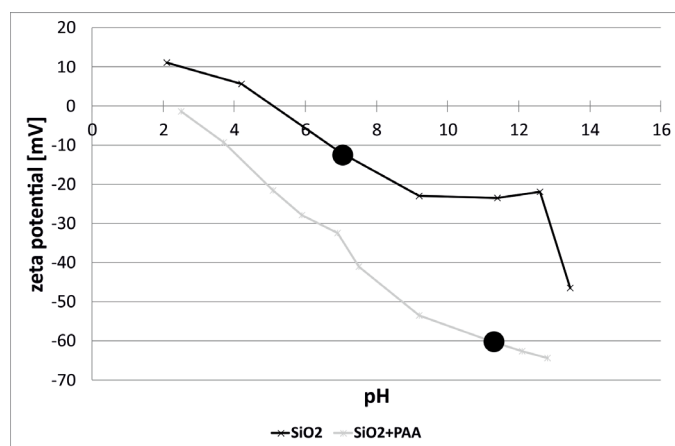

Fig. 1. Relationship between zeta potential and pH for suspensions of SiO_2 and SiO_2+PAA in ethanol
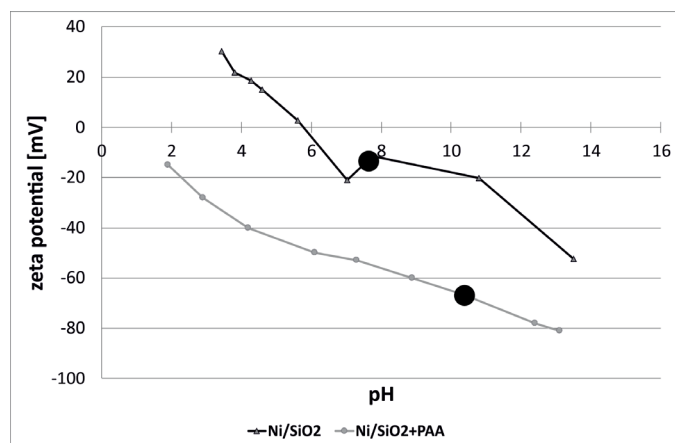

Fig. 2. Relationship between zeta potential and pH for suspensions of Ni/SiO_2 and Ni/SiO_2+PAA in ethanol

TABLE 1

Electrophoretic deposition parameters

	Chemical composition of the suspension [g/L]			pH value	Zeta potential [mV]	Applied voltage [V]	Deposition time [s]
	SiO_2	Ni	PAA				
SiO_2	1.2	—	—	6.97	−11.6	60	300
SiO_2+PAA	1.2	—	0.001	11.3	−60.3	30	180
Ni/SiO_2	1.2	15	—	7.8	−21.3	60	300
Ni/SiO_2+PAA	1.2	5	0.006	10.4	−68.1	20	180

Higher pH requires the use of large quantities of ammonia water. Increasing the concentration of water in the suspension leads to significant increase in the conductivity of the suspension, what would consequently cause the increased amount of hydrogen released on the anode. Apart from that polymer adsorption decrease with growing pH. Mutual repulsion between the growing number of dissociated –COO⁻ groups in the PAA macromolecules leads to their straightening with growing pH. The process of developing polymer chains is amplified by the weakening attraction of them to the surface and by electrostatic repulsion [21].

The increase in pH also has a significant effect on the flocculation and sedimentation of the oxide suspension [22]. Taking that into account, the pH values, that allowed to obtain macroscopic homogeneous coatings, were experimentally selected.

Suspension used for preparation of the Ni/SiO_2 coatings had pH equal to 7.8 and zeta potential equal to –21.3 mV. The addition of an anionic surfactant moved electrokinetic potential of the suspensions to more negative values. For the deposition of the coatings suspension with pH equal to 10.4 and zeta potential equal to –68.1 mV was selected, because at higher pH values, despite an increase of the stability, the coatings were deposited inhomogeneously. Probably –68.1 mV is the highest absolute value of zeta potential, at which nickel particles were uniformly deposited [23].

In order to select the optimum deposition parameters, trial series of coatings were deposited at different voltages (5 V÷90 V) and times (60 s÷420 s). It was found that macroscopically most uniform SiO_2 coatings were deposited from suspension containing 1.2 g/L of ceramic particles in ethanol, at the voltage of 60 V and deposition time equal to 300 s. The addition of PAA allowed to obtain uniform coatings at the voltage of 30 V and deposition time of 180 s.

Based on the macroscopic observations, the most homogeneous Ni/SiO_2 coatings were obtained from suspension containing 1.2 g/L of SiO_2 and 15.0 g/L of Ni in ethanol at the voltage of 60 V and deposition time of 300 s. Addition of PAA allowed the reduction of the nickel particles concentration in suspension down to 5.0 g/L, the voltage down to 20 V and the deposition time down to 180 seconds.

3.2. Microstructure of SiO_2 and Ni/SiO_2 coatings

Microstructure of the electrophoretically deposited SiO_2 and Ni/SiO_2 coatings on stainless steel are shown in Figures 3a and 3b, respectively. Both types of coatings were characterized by high homogeneity. The main drawback of these coatings was their lack of continuity. Noticeable was the large number of open pores and high amount of cracks, probably formed during drying in the air. However, these defects are typical for ceramic matrix coatings [24]. The Ni agglomerates of a few micrometres in size were randomly distributed within the coating.
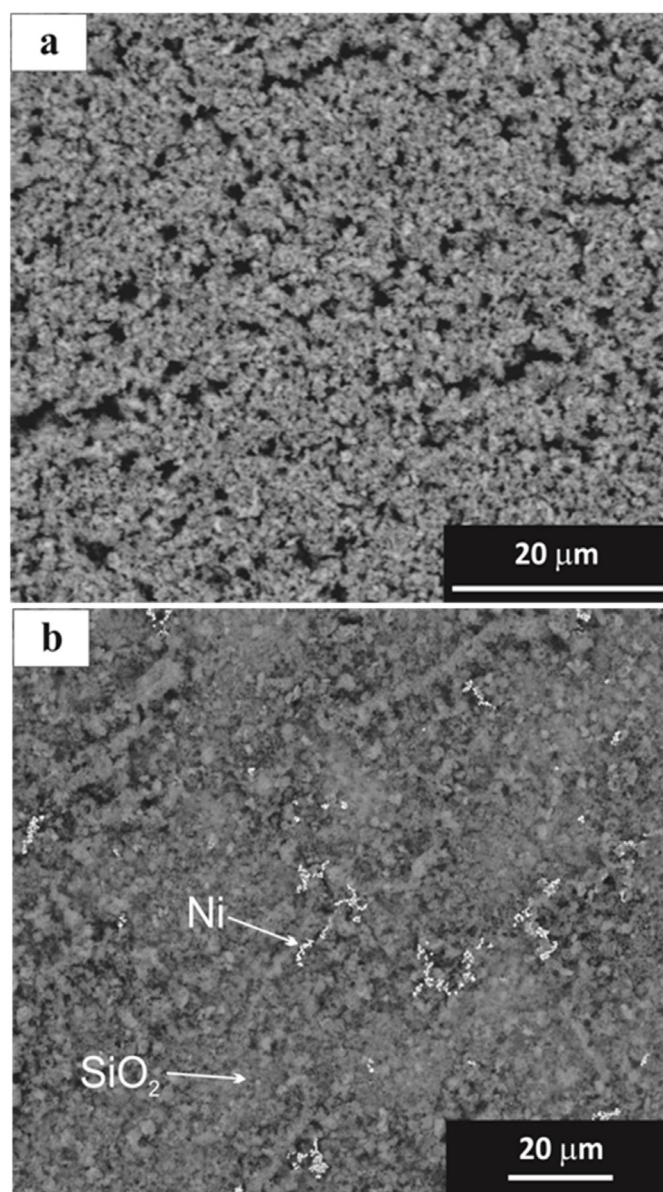

Fig. 3. SEM BSE images of the plan-view of SiO_2 (a) and Ni/SiO_2 (b) coatings on X2CrNiMo17-12-2 steel

3.3. Microstructure of SiO₂ and Ni/SiO₂ coating with PAA

Addition of the anionic surfactant increased the stability of the particles in the suspension and in consequence decreased the tendency to agglomeration. The SiO_2+PAA coating was more uniform and exhibited less amount of discontinuities (Fig. 4). Small amount of open pores was visible on the surface. These discontinuities were shallow, what can be seen on the cross-section in Fig. 5. Their presence should not adversely effect on the protective properties of the coating. Small closed pores were also present inside the coating. Formation of pores can be related with the electrostatic forces acting between ceramic particles, which disturb the uniform deposition of new particles [1]. The thickness of the SiO_2+PAA layer was uniform on the entire surface and was in the range from 4 mm to 5 mm. SiO_2 particles tightly adhered to the steel substrate but with increase of the coatings thickness, SiO_2 started deposit inhomogeneously.
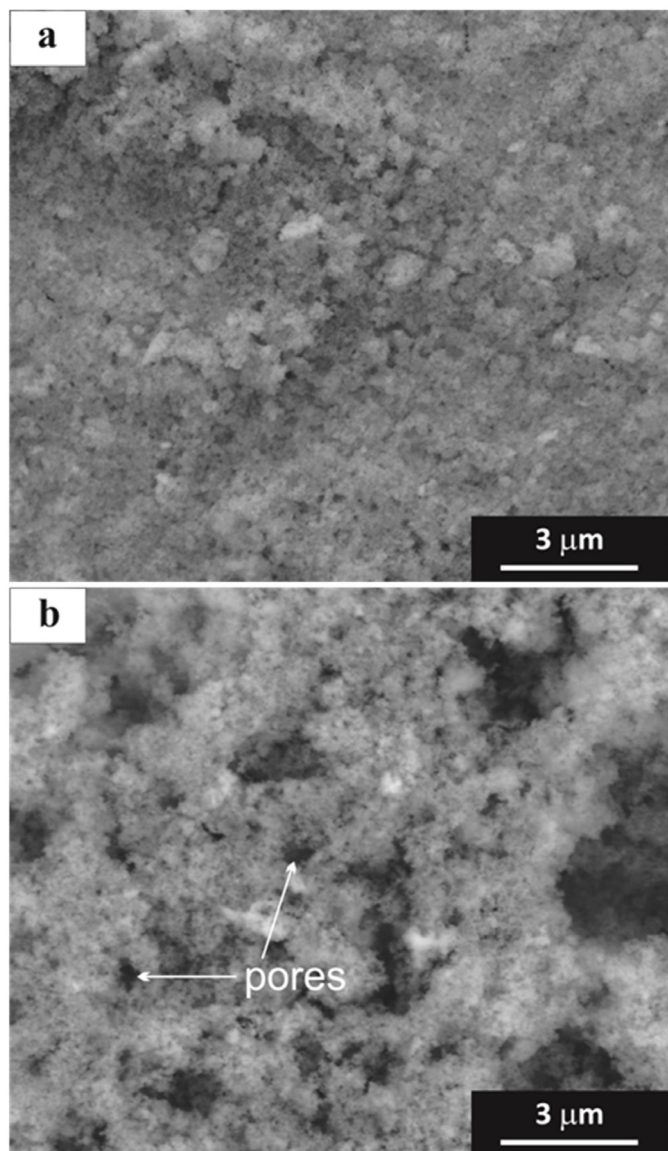
TEM microstructural analysis of SiO_2+PAA coating showed that the amorphous SiO_2 particles are closely attached to each other (Fig. 6). Such tight adherence of the nanoparticles in the coating plays a key role in ensuring a good sealing against external aggressive environment.
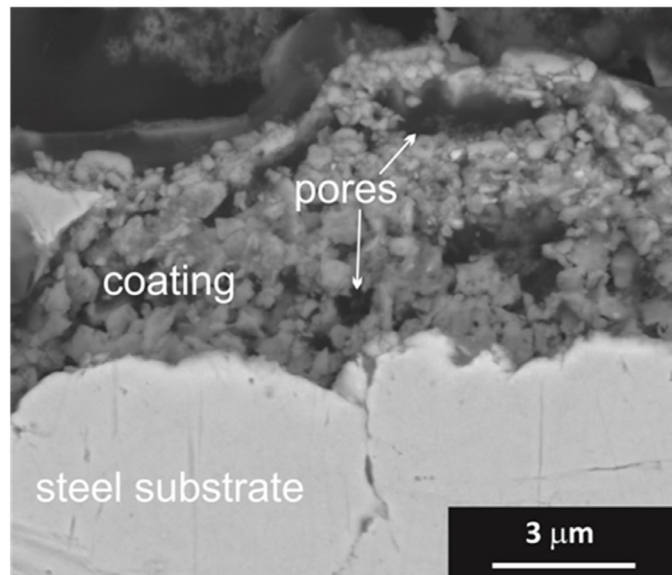

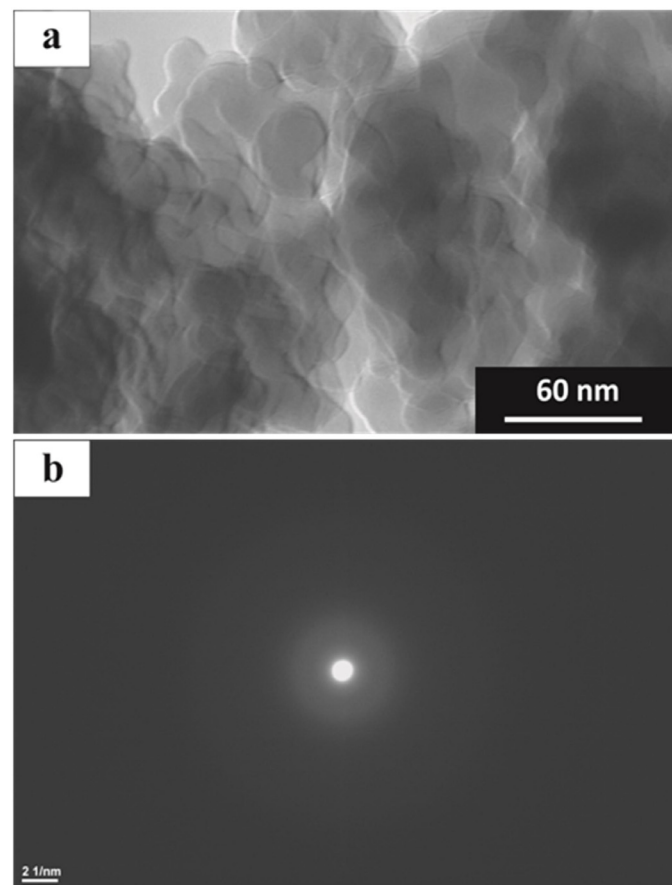Fig. 5. SEM BSE image of the cross-section of SiO_2+PAA coating on X2CrNiMo17-12-2 steel

Fig. 4. SEM (a) SE and (b) BSE images of the plan-view of SiO_2+PAA coating on X2CrNiMo17-12-2 steel

Fig. 6. Microstructure of the SiO_2+PAA coating, (a) TEM bright field, (b) SAED pattern

SEM microstructural investigation of Ni/SiO$_2$+PAA plan view specimens revealed, that the addition of 0.1 wt% of PAA to the suspension gradually decreases the presence of SiO$_2$ and Ni agglomerates in the obtained coating. Ni/SiO$_2$+PAA coating was additionally characterized by high homogeneity with small amount of open porosity (Fig. 7). Addition of PAA led to the elimination of cracks in composite coating. Slight traces of thickness variations (from 3 mm to 5 mm) in the form of waves on the coatings' surface, produced during its ascent from the suspension, were observed (Fig. 8). Similar to the SiO$_2$ coating with PAA, composite coating was characterized by good adhesion of the particles to the steel substrate. Small pores of about 1 mm in size were observed below the coatings' surface. It can be seen that all electrophoretically deposited ceramic coatings are characterized by low level of porosity, increasing with the thickness of the coatings [25].

TEM investigation of the Ni/SiO$_2$+PAA coating showed that there is a good adherence between the SiO$_2$ particles and between SiO$_2$ and Ni particles (Fig. 9a). SAED pattern and the EDS spectrum of the individual Ni particle are shown in Fig. 9b,c. The EDS maps of the Si and Ni distribution revealed that the nickel particles were uniformly distributed in the silica matrix (Fig. 9d).
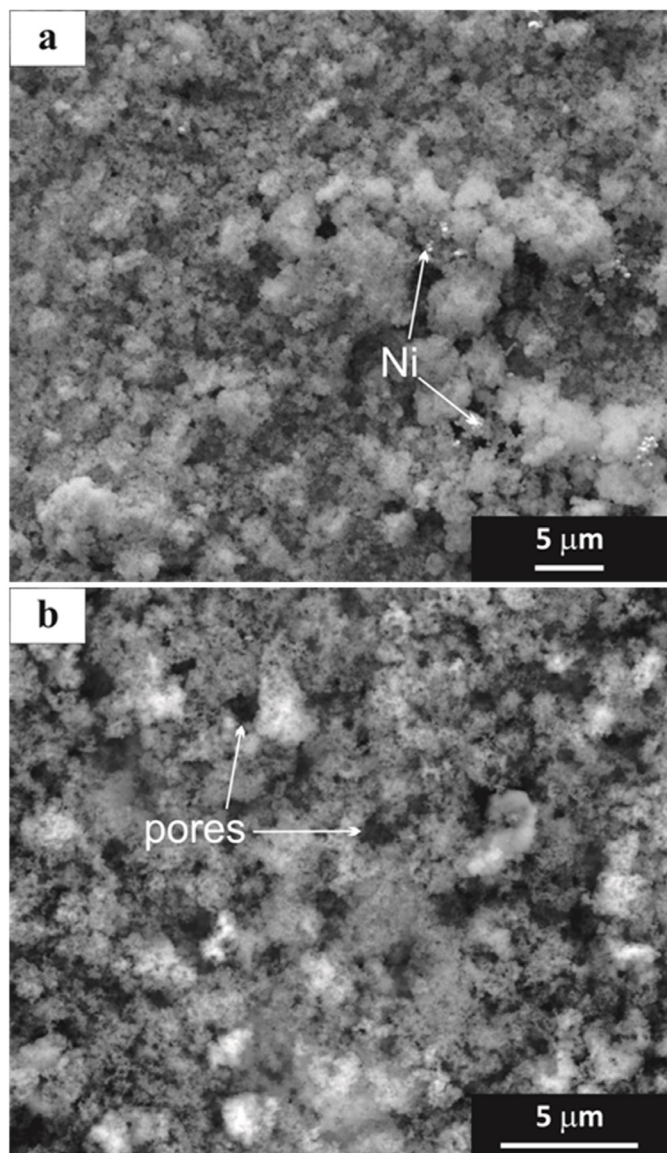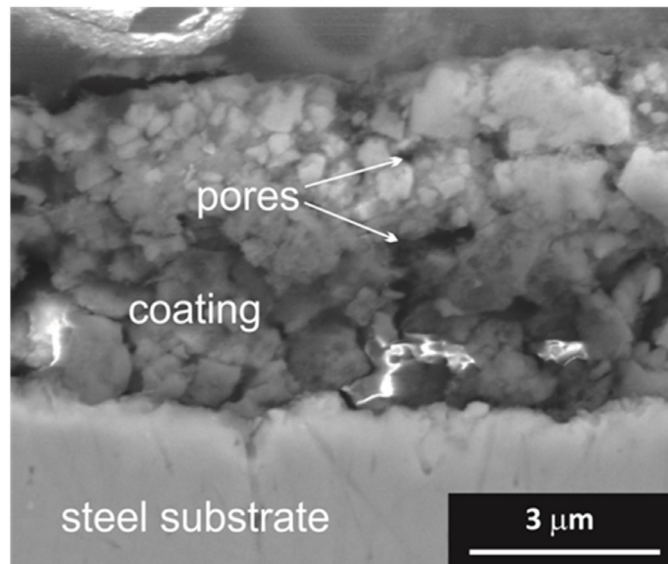

Fig. 8. SEM SE image of the cross-section of Ni/SiO$_2$+PAA coating on X2CrNiMo17-12-2 steel

3.4. Topography of the coatings

Results of the roughness measurements performed using optical profilometer are given in Table 2. The highest surface development was observed for Ni/SiO$_2$ coating. SiO$_2$ coating with addition of PAA was characterized by the smoothest surface.

TABLE 2

Surface topography parameters of the deposited coatings

	SiO$_2$	SiO$_2$+PAA	Ni/SiO$_2$	Ni/SiO$_2$+ PAA
Arithmetical mean deviation of the roughness profile (R_a) [μm]	0.8	0.4	1.5	0.5
Root mean squared (R_q) [μm]	1.3	0.7	1.9	0.7
Rverage distance between the highest peak and lowest valley (R_z) [μm]	21.2	18.3	31.5	10.5

Introduction of the PAA into the suspension influenced on the uniformity of the obtained SiO$_2$ and Ni particles distribution and thus reduction of their agglomerates, resulting in more smooth coatings surface. In both cases addition of PAA led to the decrease of all surface topography parameters. The average surface roughness R_a for SiO$_2$ and Ni/SiO$_2$ coatings on stainless steel was equal to 0.8 μm and 1.5 μm, respectively. After

Fig. 7. SEM (a) SE and (b) BSE images of the plan-view of Ni/SiO$_2$+PAA coating on X2CrNiMo17-12-2 steel
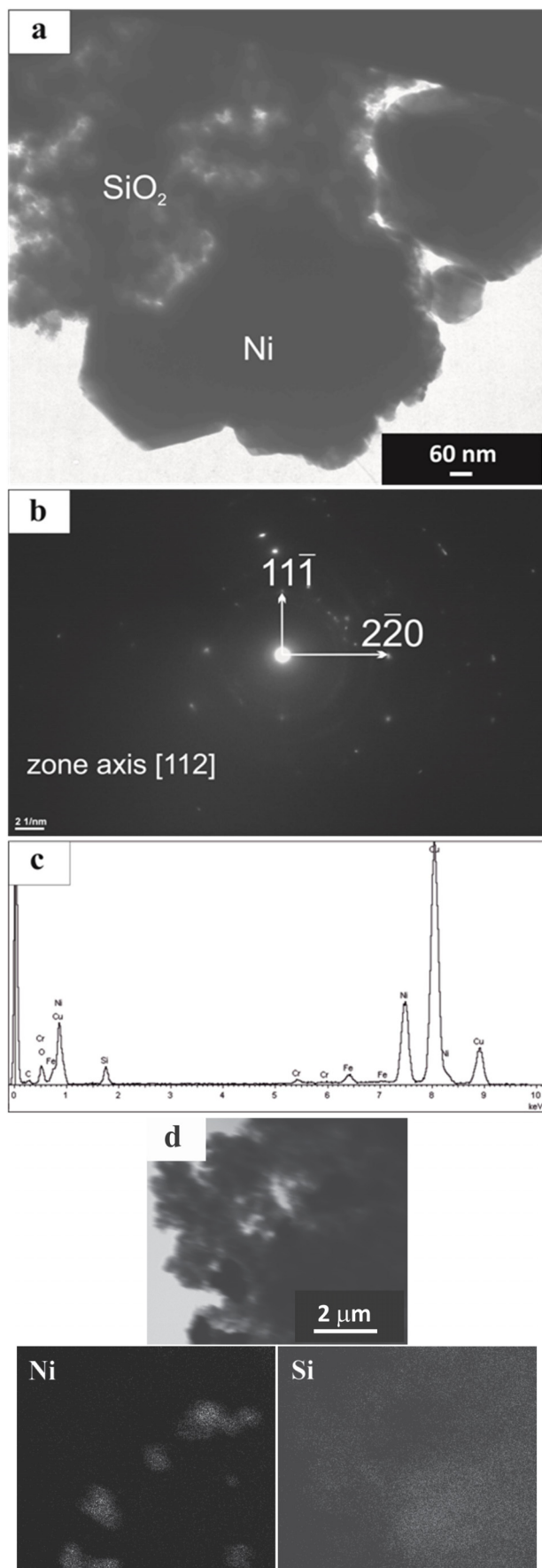
Fig. 9. Microstructure of the Ni/SiO₂+PAA coating, (a) TEM bright field, (b) SAED pattern from Ni particle area, zone axis [112]$_{Ni}$ and (c) its EDS spectrum, (d) STEM image and EDS maps showing distribution of Ni and Si in the analysed area

addition of anionic surfactant R_a of the coatings significantly decreased. It was equal to 0.4 μm and 0.5 μm for SiO₂+PAA and Ni/SiO₂+PAA, respectively. Similar effect of the anionic surfactant on the TiO₂ coatings' roughness were found in the other work [26]. In case of Ni/SiO₂ composite coating reduction of arithmetical mean deviation of the roughness profile was also found in case of addition of cationic surfactant.

3.5. Corrosion resistance

Corrosion resistance tests of the coated steel were performed using open circuit potential (OCP) measurements and polarization tests in 3.5% NaCl solution. Table 3 shows selected electrochemical parameters for uncoated X2CrNiMo17-12-2 stainless steel, coated with SiO₂ and Ni/SiO₂, and the curves for steel with the coatings with addition of PAA.

OCP measurements showed increasing values of the potential for the coated samples. This indicates a lower reactivity of the steel with ceramic and composite layers. The highest value equal to 0.07 V was observed for steel with Ni/SiO₂+PAA coating. No significant effect of the PAA on the OCP average value was observed. The difference in OCP in case of SiO₂ and Ni/SiO₂ coatings with PAA was equal to 0.02 V and 0.05 V, respectively.

For all examined materials, polarization curves profiles have similar shape (Fig. 10). Tafel plots derived from materials with coatings exhibit wider passivation regions than for uncoated steel.

TABLE 3

Selected electrochemical parameters

	I_{corr} [A]	E_{corr} [V]	Average value of OCP [V]
X2CrNiMo17-12-2 steel	2.85×10^{-5}	−0.24	−0.15
SiO₂	1.63×10^{-6}	−0.23	−0.02
SiO₂+PAA	2.89×10^{-7}	−0.13	−0.04
Ni/SiO₂	1.89×10^{-8}	−0.12	0.02
Ni/SiO₂+PAA	4.19×10^{-8}	−0.13	0.07

For Ni/SiO₂ coated steel the more electronegative corrosion potential (E_{corr}) and lower corrosion current (I_{corr}) values, as compared with the uncoated steel, were determined. The corresponding values for the Ni/SiO₂ coated steel were equal to E_{corr} = −0.12 V and I_{corr} = 1.89·10⁻⁸ A, while for the uncoated steel E_{corr} = −0.24 V and I_{corr} = 2.85·10⁻⁵. In case of SiO₂ coating, addition of 0.1 % of PAA shifted the value of E_{corr} to −0.13 V and I_{corr} to 2.89·10⁻⁷ A. This difference in corrosion parameters determined from polarisation curves was probably a consequence of the increased homogeneity and decreased number of pores in the coating due to addition of the anionic polyelectrolyte to the suspension. Based on the achieved results it can be postulated that addition of PAA to the suspension exerts positive influence on the corrosion resistance of the coatings. It is in good agreement with the results of the previous work on the effect of PAA on the

corrosion resistance of different metallic materials [26]. Umoren [27] showed that PAA inhibited the corrosion of pure cast aluminium in acidic environment. PAA multilayers decreased also susceptibility to corrosion of magnesium alloy [28]. Beside the direct influence of PAA on the corrosion resistance, its addition is also beneficial in terms of increasing the coatings' thickness and uniformity. It can have the positive impact on the resistance of the coatings against permeation of Cl^- ions.
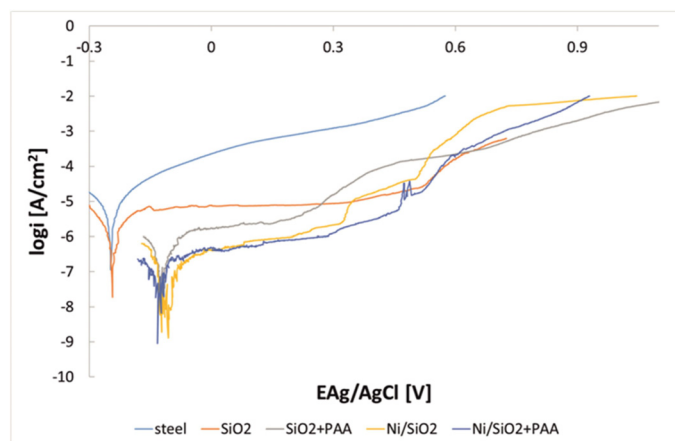

Fig. 10. Polarization curves for X2CrNiMo17-12-2 steel without coatings as well as with SiO_2 and Ni/SiO_2 coatings

4. Conclusions

1) The addition of PAA increased the zeta potential of SiO_2 and Ni particles in ethanol and thus increased the suspension stability.

2) SiO_2 and Ni/SiO_2 coatings deposited from suspensions containing PAA are characterized by the less amount of pores and desiccation cracks while compared with the coatings without PAA. TEM analysis revealed the tight adherence between SiO_2 and Ni particles within the coatings.

3) Analysis of polarization curves indicated improvement of the corrosion resistance of X2CrNiMo17-12-2 steel coated with SiO_2+PAA and Ni/SiO_2+PAA coatings in a 3.5% NaCl solution.

REFERENCES

[1] J.H. Dickerson, A.R. Boccaccini, Electrophoretic deposition of nanoparticles, Springer, 2012.

[2] J. Cho, S. Schaab, J.A. Roether, A.R. Boccaccini, J. Nanopart. Res. **10**, 99-105 (2008).

[3] Z. Weng, J. Shemilt, P. Xiao, J. Eur. Ceram. Soc. **22**, 183-189 (2002).

[4] M. Miola, E. Verne, F.E. Ciraldo, L. Cordero-Arias, A.R. Boccaccini, Front. Bioeng. Biotechnol. 3 (2015) doi: 10.3389/fbioe.2015.00159.

[5] D. Jugowiec, M. Kot, T. Moskalewicz, Arch. Metall. Mater. **61**, 657-664 (2016).

[6] S. Dor, S. Rühle, A. Ofir, M. Adler, L. Grinis, A. Zaban, Colloid. Surface. A. **342**, 70-75 (2009).

[7] Q. He, Investigation of stabilization mechanisms for colloidal suspension using nanoparticles, University of Louisville, USA (2014).

[8] G.D. Parfitt, Dispersion of Powders in Liquids, Third Edition, Applied Science, London (1981).

[9] J. Widegren, L. Bergstrom, J. Am. Cer. Soc. **85**, 523-528 (2002).

[10] S. Zafar, L.M. Negi, A.K. Verma, V. Kumar, A. Tyagi, P. Singh, Z. Igbal, S. Talegaonkar, Int. J. Pharm. **477**, 454-468 (2014).

[11] H. Yang, D. Chen, T.G.M. van de Ven, Cellulose. **22**, 1743-1752 (2015).

[12] R. Greenwood, K. Kendall, J. Eur. Ceram. Soc. **19**, 479-488 (1999).

[13] J. Hang, L. Shi, X. Feng, L. Xiao, Powder Technol. **192**, 166-170 (2009).

[14] J. Cesarano, I.A. Aksay, J. Am. Ceram. Soc. **71**, 1062-1067 (1988.)

[15] Y. Castro, B. Ferrari, R. Moreno, A. Duran, Surf. Coat. Technol. **191**, 228-235 (2005).

[16] P. De Lima Neto, M. Atik, L.A. Avaca, M.A. Aegerter, J. Sol-Gel Sci. Technol. **2**, 529-534 (1994).

[17] H. Gül, F. Kilic, S. Aslan, A. Alp, H. Akbulut, Wear **267**, 976-990 (2009).

[18] B. Xu, H. Wang, S. Dong, B. Jiang, W. Tu, B. Xu, H. Wang, S. Dong, B. Jiang, W. Tu, Electrochem. Commun. **7**, 572-575 (2005).

[19] M. Wiśniewska, J. Therm. Anal. Calorim. **101**, 753-760 (2010).

[20] X. Shi, S. Xu, J. Lin, S. Feng, J. Wang, Mater. Lett. **63**, 527-529 (2009).

[21] M. Wiśniewska, T. Urban, E. Grządka, V.I. Zarko, V.M. Gun'ko, Colloid Polym. Sci. **292** (3), 699-705 (2014).

[22] Z. Pan, A. Campbell, P. Somasundaran, Colloids Surf. A Physicochem. Eng. Asp. **191**, 71-78 (2001).

[23] E.H. Lee, M.K. Lee, C.K. Rhee, Mater. Sci. Forum **510**, 206-209 (2006).

[24] A. Charlot, X. Deschanels, G. Toquer, Thin Solid Films. **553**, 148-152 (2014).

[25] F. Shi, M.F. De Riccardis, Ceramic Coatings – Applications – Applications in Engineering, InTech, 2012.

[26] H.S. Jahromi, Int. J. Thin Film Sci. Tec. **2**, 245-260 (2013).

[27] S.A. Umoren, Y. Li, F.H. Wang, J. Solid State Electrochem. **14**, 2293-2305 (2010).

[28] L.Y. Cui, R.C. Zeng, S.Q. Li, F. Zhang, E.H. Han, RSC Adv. **6**, 63017-63116 (2016).